CrystEngComm

Accepted Manuscript

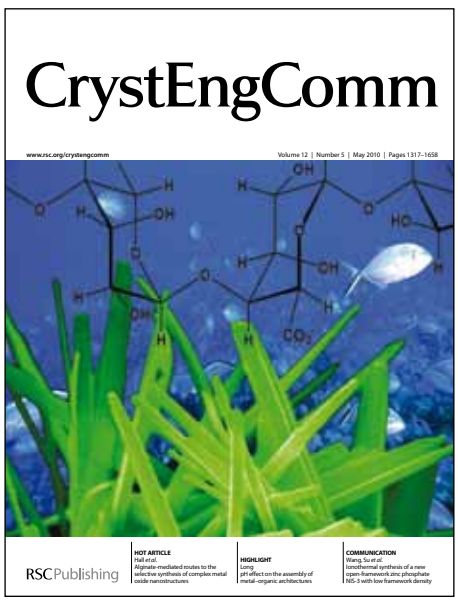

Cite this: DOI: 10.1039/c0xx00000x

www.rsc.org/xxxxxx

Paper

Coordination Polymers of a Multipyridyl and Pyrazolyl Ligand with Conformational Flexibility: Syntheses, Structures and Luminescence

Caixia Ding, Xing Rui, Cheng Wang and Yongshu Xie*

Received (in XXX, XXX) Xth XXXXXXXXX 20XX, Accepted Xth XXXXXXXXX 20XX

DOI: 10.1039/b000000x

In this work, we designed and synthesized a novel ligand N,N-bis(6-(1H-pyrazolyl)2-pyridyl)-N',N'-bis(4-pyridyl)1,4-phenylenediamine (L). Coordination of d^{10} metals, Co(II), and Cu(II) with L generated eight novel coordination polymers $[ZnLCl_2]_n$ (**1**), $[ZnLBr_2]_n$ (**2**), $[ZnLI_2]_n$ (**3**), $[CdL_2Cl_2]_n$ (**4**), $[CdL_2Br_2]_n$ (**5**), $[CdLI_2]_n$ (**6**) $\{[CoL(SCN)](ClO_4)\}_n \cdot 1.5nDMF \cdot 0.5nH_2O$ (**7**) and $\{[Cu_2L_2(N_3)]\cdot 3ClO_4\}_n$ (**8**). Single-crystal X-ray diffraction analyses revealed that complexes **1-3** and **6** are isostructural. In these complexes, the ligand L utilizes its two pyridyl nitrogens of the 4,4'-dpa moiety to bridge metal ions, affording 1D zigzag chains, which are further linked by intermolecular C−H···π and hydrogen bond interactions to form 3D supramolecular structures. Complexes **4** and **5** have isostructural 1D double chain structures. In the d^{10} metal complexes **1-6**, the potentially chelating bppa units of L are left non-coordinated in the "L" or "M" shaped conformation. In contrast, in complexes **7** and **8**, the bppa units chelate the paramagnetic metal ions in the "U" shaped conformation. For complex **7**, the bppa unit of L chelates a Co(II) atom, and a pyridyl nitrogen of the 4,4'-dpa unit bridges another Co(II) atom, thus, affording a 1D chain structure. Similar to that observed in **7**, each L ligand in complex **8** links two Cu(II) ions, and a $\mu_{1,3}$-azide further bridges two Cu(II) ions from neighbouring chains, affording a 2D undulated layer, which is interpenetrated by another such 2D sheet, forming a 2-fold interpenetrated structure. Based on the interesting structural results, the solid state luminescent properties of complexes **1-6** were investigated, which revealed that the emission maxima wavelengths can be tuned in a large range of 372−486 nm.

Introduction

Functional coordination polymers have attracted considerable attention because of the intriguing structures and properties with potential applications in various areas such as gas absorption, catalysis, luminescence and magnetism.[1-3] It is noteworthy that coordination polymers containing d^{10} metal ions, especially those of zinc(II) and cadmium(II) provide a powerful platform for the development of solid-state luminescent materials, and the luminescent behavior can be readily tuned by the variation of the metal ions and the organic ligands.[4-6]

Regarding the organic ligands, both bridging and chelating pyridyl moieties, such as 2,2′-dipyridylamine (2,2′-dpa), 4,4′-dipyridylamine (4,4′-dpa) and their derivatives,[7-8] have been intensely investigated due to the strong coordination ability and structural diversity. In this respect, we have designed various polypyridyl ligands containing 4,4′-dpa and 2,2′-dpa moieties (L[1]~L[3], Scheme 1). These ligands may coordinate with up to four metal centers to afford coordination polymers with a rich structural diversity and interesting solid state emissions.[9] In spite of this, none of these complexes show the chelation of the 2,2′-dpa moiety, which may be attributed to the relatively weak chelating ability of the amino N-linked 2,2′-dpa unit. In order to strengthen the chelating ability, two pyrazole units were introduced into the 2,2′-dpa moiety at the 6 and 6′ positions to afford a novel tetradentate coordinating moiety, bis(6-(1H-pyrazolyl)-2-pyridyl)amine (bppa), which was further combined with a 4,4′-dpa moiety to afford a novel multidentate ligand L (Scheme 1). The coordination of L with Zn(II) and Cd(II) afforded a series of coordination polymers: $[ZnLCl_2]_n$ (**1**), $[ZnLBr_2]_n$ (**2**), $[ZnLI_2]_n$ (**3**), $[CdL_2Cl_2]_n$ (**4**), $[CdL_2Br_2]_n$ (**5**), $[CdLI_2]_n$ (**6**). In these complexes, the bppa unit did not chelate the metal ions. These observations may be related to the coordination preferences of the d^{10} metal ions. Thus, we continued to use Co(II) and Cu(II) to coordinate with L to afford coordination polymers $\{[CoL(SCN)](ClO_4)\}_n \cdot 1.5nDMF \cdot 0.5nH_2O$ (**7**) and $\{[Cu_2L_2(N_3)]\cdot 3ClO_4\}_n$ (**8**). As expected, the bppa units demonstrated the chelating mode in these complexes.

The photoluminescence of the L ligand and complexes **1-6** in the solid state was also measured and discussed on the basis of the structural results.

Key Laboratory for Advanced Materials and Institute of Fine Chemicals, East China University of Science & Technology, Shanghai 200237, P. R. China. E-mail: yshxie@ecust.edu.cn

† Electronic Supplementary Information (ESI) available: X-ray crystallographic files (CIF format), selected bond lengths and angles for complexes and part figures. CCDC reference numbers 968017-968025. See DOI: 10.1039/b000000x/

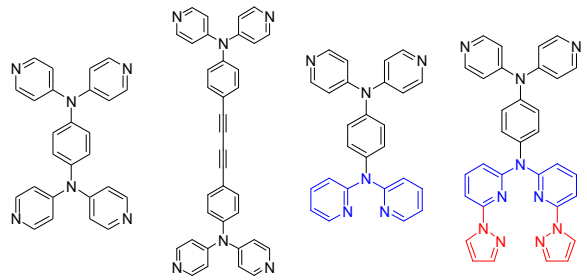

(L^1) (L^2) (L^3) (L)

Scheme 1 Structures of L and related polypyridyl ligands

Experimental Section

Materials. All chemicals of reagent grade quality were used as received from commercial sources. (4-Bromophenyl)-bis(4-pyridyl)amine[9] and **D1**[10] were prepared as we previously reported.

Physical measurements. ^{1}H NMR spectra were recorded on a Bruker AVANCE spectrometer (400 MHz). FT-IR spectra were recorded in the region of 400-4000 cm^{-1} on a Thermo Electron Avatar 380 FT-IR instrument (KBr Discs). Elemental analyses were carried out with an Elmentar Vario EL-III analyzer. Fluorescence measurements were performed on a Varian Cary Eclipse fluorescence spectrophotometer. HRMS were performed using a Waters LCT Premier XE spectrometer.

Syntheses and crystal growth.

D2: A mixture of pyrazole (10 g, 146.8 mmol), **D1** (3 g, 9.1 mmol), CuI (570 mg, 3.0 mmol) and Cs_2CO_3 (7 mg, 21.5 mmol) was degassed and flushed with nitrogen. The mixture was stirred at 110°C for 24 h. After cooling, 50 mL dichloromethane was added into the reaction mixture, and the precipitate was filtered off and washed with dichloromethane. The filtrates were evaporated in vacuo. The residue was purified by column chromatography to afford compound **D2** as a yellowish solid (2.45 g, 89% yield). ^{1}H NMR (DMSO-d_6, Bruker 400 MHz), δ: 10.08 (s, 1H, NH), 8.57 (d, 2H, J = 2.0 Hz), 7.92 (m, 2H), 7.83 (d, 2H, J = 0.8 Hz), 7.66 (d, 2H, J = 8.0 Hz), 7.44 (d, 2H, J = 7.6 Hz), 6.61 (m, 2H). ^{13}C NMR (DMSO-d_6, Bruker 100 MHz, 298K), δ:157.93, 154.43, 147.21, 146.06, 132.06, 114.59, 113.23, 108.62. HRMS: obsd 304.1310, calcd for $C_{16}H_{14}N_7$ ([M+H]$^+$): 304.1311.

L: **D2** (2.1 g, 6.9 mmol) was dissolved in diphenyl ether (150 mL), and then (4-bromophenyl)-bis(4-pyridyl)amine (3.8 g, 11.7 mmol), $CuSO_4$ (264 mg, 1.6 mmol), K_2CO_3 (960 mg, 6.9 mmol) and 18-crown-6 (132 mg, 0.3 mmol) were added. The mixture was heated at 170°C under N_2 for 3 days. After the reaction was cooled, the diphenyl ether was removed by distillation under reduced pressure. The residue was purified by a silica gel column to afford a colorless solid of the ligand **L** (1.6 mg, 42% yield). ^{1}H NMR (d_6-DMSO, Bruker 400 MHz), δ: 8.45 (d, 4H, J= 6.4 Hz), 8.09 (d, 2H, J= 2.4 Hz), 7.95 (t, 2H, J= 8.0 Hz), 7.81 (s, 2H), 7.57 (d, 2H, J= 8.0 Hz), 7.44 (d, 2H, J= 8.8 Hz), 7.35 (d, 2H, J= 8.8 Hz), 7.16 (d, 2H, J= 8.0 Hz), 7.05 (d, 4H, J= 6.0 Hz), 6.55 (t, 2H, J= 2.0 Hz). HRMS: obsd 549.2267, calcd for $C_{32}H_{25}N_{10}$ ([M+H]$^+$): 549.2264.

$[ZnLCl_2]_n$ (1) A mixture of **L** (5.5 mg, 0.01 mmol) and $ZnCl_2$ (2.7 mg, 0.02 mmol) in DMF and MeCN (2:9) was sealed in a small vial (10 ml), which was heated to 120°C for 120 h. After cooling to room temperature, yellowish crystals of **1** suitable for

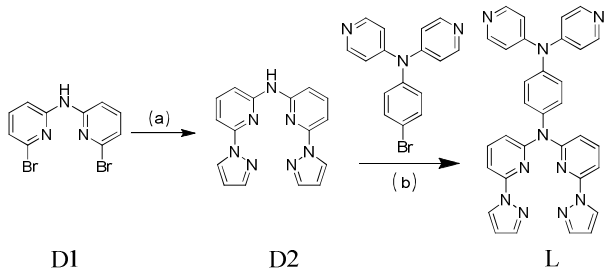

D1 D2 L

Scheme 2 Synthesis of L. Reaction conditions: (a) pyrazole, Cs_2CO_3, CuI, (b) $CuSO_4$, K_2CO_3, 18-crown-6, Ph_2O.

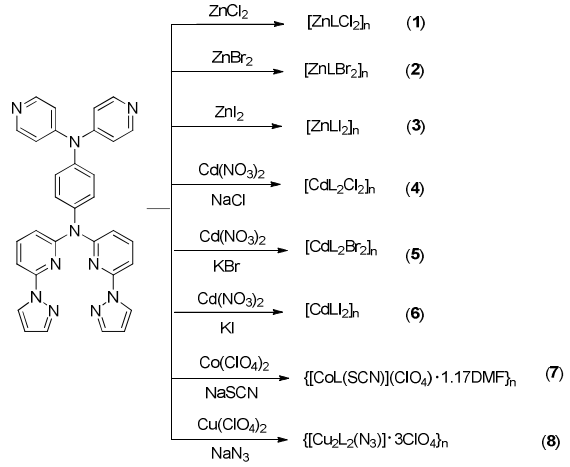

Scheme 3 Syntheses of complexes **1**-**8**.

X-ray structure determination were obtained. Yield: 4 mg, 63%. Anal. (%) calcd. for $C_{32}H_{24}Cl_2N_{10}Zn$: C, 56.12; H, 3.53; N, 20.45. Found: C, 56.03; H, 3.57; N, 20.39. IR (KBr pellet, cm^{-1}): 3432(br), 2920(w), 1597(s), 1570(s), 1504(s), 1489(s), 1447(s), 1414(m), 1392(m), 1347(m), 1314(m), 1215(w), 1199(m), 1149(w), 1063(w), 1025(s), 826(w), 797(m), 763(m), 647(m).

$[ZnLBr_2]_n$ (2) Compound **2** was prepared by a procedure similar to that for **1**, using $ZnBr_2$ (4.5 mg, 0.02 mmol) in place of $ZnCl_2$. Yellowish block crystals of **2** were obtained. Yield: 5 mg, 65%. Anal. (%) calcd. for $C_{32}H_{24}Br_2N_{10}Zn$: C, 49.67; H, 3.13; N, 18.10. Found: C, 49.54; H, 3.19; N, 18.21. IR (KBr pellet, cm^{-1}): 3415(br), 1617(m), 1599(s), 1500(s), 1450(s), 1394(m), 1349(m), 1317(m), 1294(w), 1217(w), 1203(w), 1149(m), 1026(m), 986(m), 794(w), 768(w), 628(w).

$[ZnLI_2]_n$ (3) Compound **3** was prepared by a procedure similar to that for **1**, using ZnI_2 (6.3 mg, 0.02 mmol) in place of $ZnCl_2$. Yellowish block crystals of **3** were obtained. Yield: 4 mg, 46%. Anal. (%) calcd. for $C_{32}H_{24}I_2N_{10}Zn$: C, 44.29; H, 2.79; N, 16.14; Found: C, 44.34; H, 2.69; N, 16.08. IR (KBr pellet, cm^{-1}): 3416(br), 1599(s), 1570(s), 1503(s), 1453(s), 1410(m), 1392(s), 1348(s), 1317(m), 1292(m), 1254(w), 1216(m), 1148(m), 1064(m), 1041(m), 1025(s), 928(w), 825(m), 795(m), 766(s), 703(w), 643(m), 543(w).

$[CdL_2Cl_2]_n$ (4) A mixture of **L** (5.5 mg, 0.01 mmol), $Cd(NO_3)_2{\cdot}4H_2O$ (6.2 mg, 0.02 mmol), and NaCl (2.2 mg, 0.04 mmol) in MeOH and H_2O (20:5) was sealed in a 10 ml Teflon lined stainless steel vessel under autogenous pressure and heated to 150°C for 100 h. After cooling to room temperature, colorless

crystals of **4** were obtained. Yield: 3 mg, 47%. Anal. (%) calcd. for $C_{64}H_{48}CdCl_2N_{20}$: C, 60.03; H, 3.78; N, 21.88. Found: C, 60.15; H, 3.67; N, 21.94. IR (KBr pellet, cm^{-1}): 3549(m), 3475(s), 3414(s), 1597(s), 1583(s), 1491(m), 1447(vs), 1413(m), 1394(w), 1343(w), 1307 (s), 1217(w), 1200(w), 1040(w), 1001(w), 936(w), 789(m), 675(m), 639(m).

$[CdL_2Br_2]_n$ (5) Compound **5** was prepared by a procedure similar to that for **4**, using KBr (4.7 mg, 0.04 mmol) in place of NaCl. Colorless crystals of **5** were obtained. Yield: 4 mg, 59%. Anal. (%) calcd. for $C_{64}H_{48}Br_2CdN_{20}$: C, 56.13; H, 3.53; N, 20.46. Found: C, 56.25; H, 2.87; N, 10.53. IR (KBr pellet, cm^{-1}): 3414(br), 1597(s), 1582(vs), 1490(m), 1446(s), 1413(m), 1343(m), 1307(s), 1217(m), 1200(w), 11148(w), 1039(w), 1003(m), 936(w), 811(w), 789(m), 752(m), 639(m), 477(w).

$[CdLI_2]_n$ (6) Compound **6** was prepared by a procedure similar to that for **4**, using KI (6.6 mg, 0.04 mmol) in place of NaCl Colorless crystals of **6** were obtained. Yield: 6 mg, 66%. Anal. (%) calcd. for $C_{32}H_{24}CdI_2N_{10}$: C, 42.01; H, 2.64; N, 15.31.Found: C, 42.13; H, 2.69; N, 15.22. IR (KBr pellet, cm^{-1}): 3414(br), 1593(s), 1499(m), 1450(s), 1410(m), 1410(m), 1392(s), 1348(s), 1317(m), 1293(m), 1254(w), 1217(m), 1202(w), 1148(w), 1063(w), 1041(m), 1017(m), 928(w), 823(m), 795(m), 765(m), 703(w), 641(m), 534(w).

$\{[CoL(SCN)](ClO_4)\}_n \cdot 1.5nDMF \cdot 0.5nH_2O$ (7) A mixture of **L** (5.5 mg, 0.01 mmol), $Co(ClO_4)_2 \cdot 6H_2O$ (7.3 mg, 0.02 mmol), and NaSCN (1.6 mg, 0.02 mmol) in DMF and H_2O (15:4) was sealed in a 10 ml Teflon lined stainless steel vessel under autogenous pressure and heated to 150°C for 100 h. After cooling to room temperature, pink crystals of **7** were obtained. Yield: 2 mg, 21%. Anal. (%) calcd. for $C_{75}H_{70}Cl_2Co_2N_{25}O_{12}S_2$: C, 51.00; H, 3.99; N, 19.82;. Found: C, 50.75; H, 3.81; N, 20.04. IR (KBr pellet, cm^{-1}): 3436(br), 3126(m), 2071(vs), 1663(s), 1582(vs), 1497(s), 1459(s), 1437(s), 1404(m), 1339(w), 1316 (w), 1264(w), 1213(w), 1186(w), 1085(vs), 985(m), 787(m), 621(m), 542(m).

$\{[Cu_2L_2(N_3)]\cdot 3ClO_4\}_n$ (8) Compound **8** was prepared by a procedure similar to that for **7**, using $Cu(ClO_4)_2 \cdot 6H_2O$ (7.4 mg, 0.02 mmol) and NaN_3 (1.3 mg, 0.02 mmol) in place of $Co(ClO_4)_2 \cdot 6H_2O$ and NaSCN. Dark green crystals of **8** were obtained. Yield: 2 mg, 25%. Anal. (%) calcd. for $C_{64}H_{48}Cl_3Cu_2N_{23}O_{12}$: C, 49.13; H, 3.09; N, 20.59. Found: C, 49.26; H, 2.97; N, 20.71. IR (KBr pellet, cm^{-1}): 3415(br), 3129(w), 2048(vs), 1585(s), 1494(m), 1468(s), 1442(m), 1409(m), 1384(w), 1344(w), 1317(m), 1269(m), 1254(w), 1217(m), 1121(m), 1088(s), 1024(w), 999(m), 787(m), 623(w), 543(w).

X-ray Crystallography. X-Ray diffraction data were collected on a Bruker-AXS APEX diffractometer utilizing MoKα radiation (λ=0.71073 Å). The structures were solved by direct methods and refined with full-matrix least-squares technique. Anisotropic thermal parameters were applied to all non hydrogen atoms. All of the hydrogen atoms in these structures are located from the differential electron density map and constrained to the ideal positions in the refinement procedure. All calculations were performed using SHELX-97 software package.[11] Crystal data and experimental details for the crystals are summarized in Table 1, and selected bond lengths and bond angles are given in Table S1.

Table 1. Crystallographic data and structure refinements summary for L and complexes **1**-**8**.

Compounds	**L**	**1**	**2**	**3**	**4**	**5**	**6**	**7**	**8**
Empirical formula	$C_{32}H_{24}N_{10}$	$C_{32}H_{24}Cl_2N_{10}Zn$	$C_{32}H_{24}Br_2N_{10}Zn$	$C_{32}H_{24}I_2N_{10}Zn$	$C_{64}H_{48}CdCl_2N_{20}$	$C_{64}H_{48}Br_2CdN_{20}$	$C_{32}H_{24}CdI_2N_{10}$	$C_{75}H_{70}Cl_2Co_2N_{25}O_{12}S_2$	$C_{64}H_{48}Cl_3Cu_2N_{23}O_{12}$
Fw	548.61	684.88	773.80	867.78	1280.52	1369.44	914.81	1766.44	1564.68
Crystal System	Monoclinic	Orthorhombic	Monoclinic	Monoclinic	Monoclinic	Monoclinic	Monoclinic	Monoclinic	Monoclinic
Space group	P2(1)/c	Pca2(1)	P2(1)/n	P2(1)/n	P2(1)/c	P2(1)/n	P2(1)/n	C2/c	C2/c
T (K)	298(2) K	298(2)	298(2)	293(2)	298(2)	293(2)	298(2)	298(2)	293(2)
a (Å)	18.3083(18)	19.6653	10.2118(9)	10.5859(7)	7.8210(5)	7.9001(7)	10.8437(11)	36.645(3)	34.166(3)
b (Å)	6.8191(5)	11.3358(11)	18.3727(17)	16.9380(14)	44.970(3)	44.620(3)	16.6662(16)	8.7390(6)	8.5280(9)
c (Å)	22.558(2)	14.1097(12)	18.2062(16)	19.398(2)	11.0991(9)	8.0308(4)	19.6797(18)	25.427(2)	24.721(2)
β (deg)	101.5190(10)	90	96.2340(10)	96.5450(10)	134.490(2)	91.642(2)	96.6390(10)	104.3040(10)	99.831(2)
V ($Å^3$)	2759.5(4)	3145.4(5)	3395.6(5)	3455.5(5)	2784.8(3)	2829.7(3)	3532.7(6)	7890.4(10)	7096.9(12)
Z	4	4	4	4	2	2	4	4	4
D_{calcd} (Mg/m^3)	1.321	1.446	1.514	1.668	1.527	1.607	1.720	1.487	1.464
μ (mm^{-1})	0.084	0.991	3.114	2.535	0.553	1.862	2.403	0.620	0.789
no. of reflns ($I>2\sigma(I)$)	4854	4768	5355	6065	4909	5000	6222	6953	6228
Final R_1[a][$I>2\sigma(I)$]	0.0444	0.0639	0.0865	0.0818	0.0782	0.0541	0.0513	0.0620	0.0582
wR_2[b] (all data)	0.1061	0.1952	0.2488	0.2499	0.1932	0.1215	0.1444	0.1753	0.1882
Goodness of fit	1.031	1.051	0.881	1.023	1.178	1.059	1.091	1.067	1.072

[a] $R_1 = \Sigma||F_o| - |F_c||/\Sigma|F_o|$. [b] $wR_2 = [\Sigma[w(F_o^2 - F_c^2)^2]/\Sigma[w(F_o^2)^2]]^{1/2}$

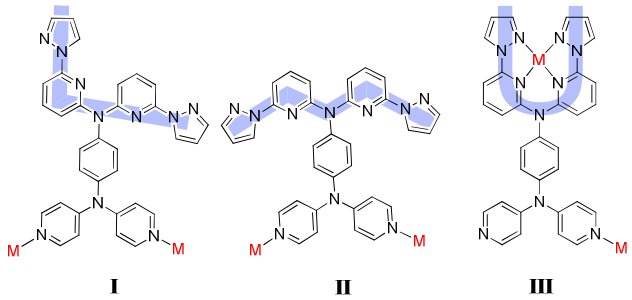

Scheme 4. Various coordination modes of L in complexes **1-8** with the bppa moieties in the conformations of "L", "M", and "U".

Results and discussion

Synthesis and characterization

The synthetic route for ligand L is summarized in Scheme 2. The amino intermediate D2 was synthesized from D1 and pyrazole by an Ullmann coupling reaction with CuI and Cs_2CO_3 used as the catalyst and the base, respectively. D2 was obtained in a high yield of 89% after purification by column chromatography on silica gel. The ligand L was prepared in a moderate yield from an Ullmann condensation reaction of D2 with (4-bromophenyl)-bis(4-pyridyl)amine at 170˚C in diphenyl ether, using cupric sulfate and K_2CO_3 as the catalyst and the base, respectively (Scheme 2). The single crystals of L were obtained by slow evaporation of the MeOH solution at room temperature.

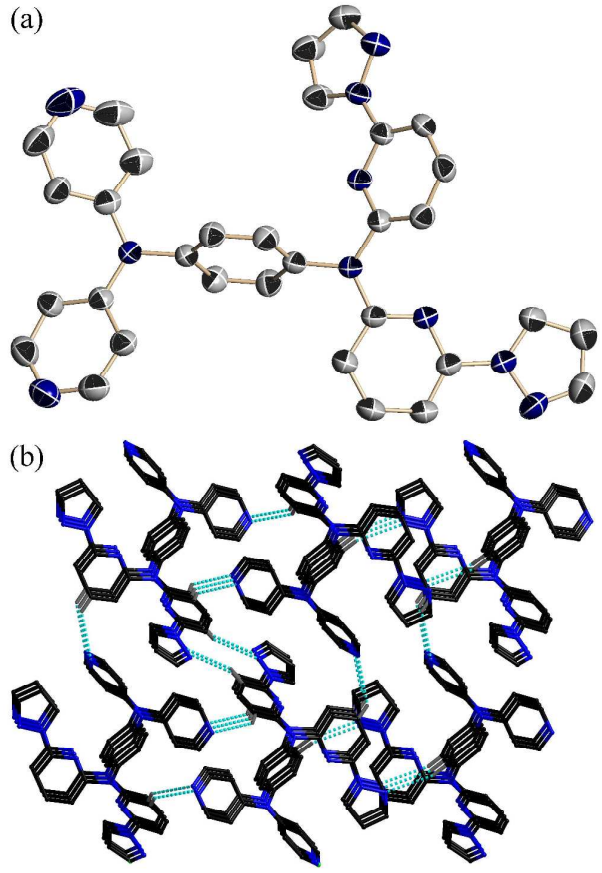

Fig 1. (a) Molecular structure of ligand L with thermal ellipsoids shown at the 50% probability level. Hydrogen atoms are omitted for clarity. (b) 3-D structure of L showing intermolecular hydrogen bonds.

Then, L was utilized to coordinate with Zn(II), Cd(II), Co(II) and Cu(II) salts under the solvothermal conditions, affording complexes **1-8**. The ligand and complexes were characterized by elemental analyses and IR spectra. In the IR spectrum of **7**, the appearance of a strong band at 2071 cm^{-1} indicates the presence of terminally coordinated SCN^- groups,[12] which is consistent with the crystal structure (*vide infra*). The existence of N_3^- group in complex **8** is clearly demonstrated by the presence of strong characteristic peak at 2048cm^{-1}. The ClO_4^- peaks appear at 1085 and 1088 cm^{-1} for **7** and **8**, respectively. These peaks are indicative of free perchlorate anions, which are in agreement with the crystal structures (*vide infra*). To further understand the structures of these complexes, the single crystals were grown and analyzed by X-ray diffraction.

Crystal structure of L

Crystal structure of L is shown in Fig.1. The molecule is deviated from a planar structure due to the steric hindrance effect. The angles between the central phenylene unit and the four pyridyl rings lie in the range of 66.6(3)-78.9(3)˚. It is noteworthy that the conformation of the bppa moiety looks like the letter "L" with a vertical branch and a horizontal branch (Fig.1a).

Weak intramolecular hydrogen bonds occur between the pyridyl/phenyl CH and the pyridyl/pyrazolyl N atoms, with H···N and C···N distances varying in the ranges of 2.69~2.72 and 3.411(1)~3.594(1) Å, respectively. The C-H···N angles lie in the range of 132~160°. By the linkage of such intermolecular hydrogen bonds, a 3D supramolecular structure is formed (Fig. 1b).

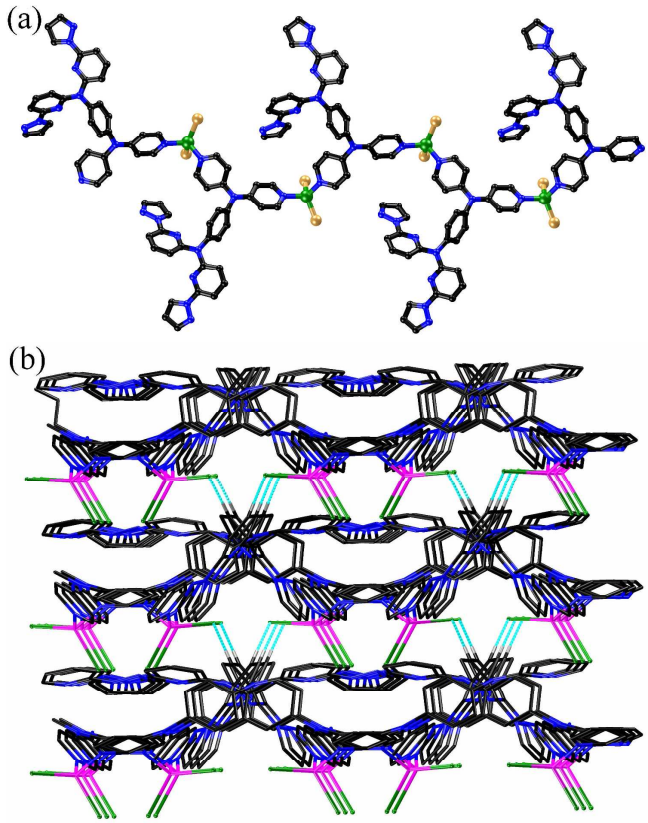

Fig 2. (a) 1D chain of complex **1**, (b) Three-dimensional supramolecular structure formed by hydrogen bond interactions.

Crystal structure of $[ZnLCl_2]_n$ (1)

The asymmetric unit of crystal **1** consists of one Zn(II) atom, one L ligand and two chlorine anions. Each Zn(II) atom is located in a distorted tetrahedral coordination environment, provided by two chlorines and two pyridyl nitrogens. The average bond lengths of Zn-N and Zn-Cl are 2.027(9) and 2.227(3) Å, respectively. L utilizes its two pyridyl nitrogens of the 4,4'-dpa moiety to bridge two Zn(II) atoms, affording a zigzag-like chain with the bppa moiety left non-coordinated, adopting the same "L" conformation as that observed in the crystal of the ligand (Fig. 2a).

Furthermore, the H···Cl distance (2.78 Å) between the pyridyl CH and the chlorine atoms from neighboring chains is shorter than the sum of the van der Waals radii for H and Cl (ca. 1.2 Å for H, 1.75 Å for Cl),[13] and the C-H···Cl angle is 163˚, which indicates a typical intermolecular hydrogen bond between the neighboring chains. By linkage of the interchain hydrogen bonds, a 3D supramolecular structure is formed (Fig.2b).

Crystal structure of $[ZnLBr_2]_n$(2), $[ZnLI_2]_n$ (3) and $[CdLI_2]_n$ (6) The structure of complex **2** is shown in Fig. 3, and complexes **3** and **6** are isostructural to **2**. In complexes **2** and **3**, each Zn is tetracoordinated with a distorted tetrahedral coordination environment. The average Zn-N distances for **2** and **3** are 2.033(9) and 2.060(9) Å, respectively, which are larger than that of 2.027(9) Å for complex **1**. This result may be attributed to the differences in the anion radius. The larger radius can induce more severe steric hindrance, and thus the Zn-N distances increase with the increase of the anion radius. On the other hand, the average Zn-Br and Zn-I distances are 2.369(2) and 2.547(2) Å, respectively, which lie within the normal bond length ranges reported previously.[14] Similarly, each Cd(II) atom in complex **6** also adopts the distorted tetrahedral coordination environment with the average Cd-N and Cd-I bond lengths of 2.286(5) and 2.687(8) Å, respectively.

Complexes **2**, **3** and **6** also exhibit zigzag chains similar to that of complex **1**, except that the bppa moieties in these three complexes have two horizontally aligned branches, just like the letter "M" (mode II, Scheme 4).

In complex **2**, the zigzag chains are linked by intermolecular hydrogen bonds between the 4,4'-dpa pyridyl CH and pyridyl N atoms of the bppa moieties from neighboring chains, with C···N distances of 3.306(2) Å, and the C–H···N angles of 127˚, thus affording a 2D network (Fig. 3b). Furthermore, the interlayer C-H···Br hydrogen bonds between the phenyl CH and Br atoms from adjacent layers are observed. The H···Br distance is 2.80 Å and the C–H···Br angle is 150˚, which lie in the normal range as previously reported.[13] Finally, a 3D supramolecular structure is formed (Fig. 3c).

Crystal structure of $[CdL_2Cl_2]_n$ (4) and $[CdL_2Br_2]_n$ (5)

Single crystal X-ray analyses revealed that complexes **4** and **5** are isostructural. And the structures are obviously different from those of complexes **1**-**3** and **6**. Complex **4** crystallizes in a monoclinic system with space group P2(1)/c and the asymmetric unit contains one Cd(II) atom, one Cl^- anion and an L ligand. Each Cd(II) has a distorted octahedral coordination geometry, with four pyridyl nitrogens from four L ligands coordinated in the equatorial plane and two chlorides coordinated at the axial positions. The Cd-N bond lengths lie in the range of

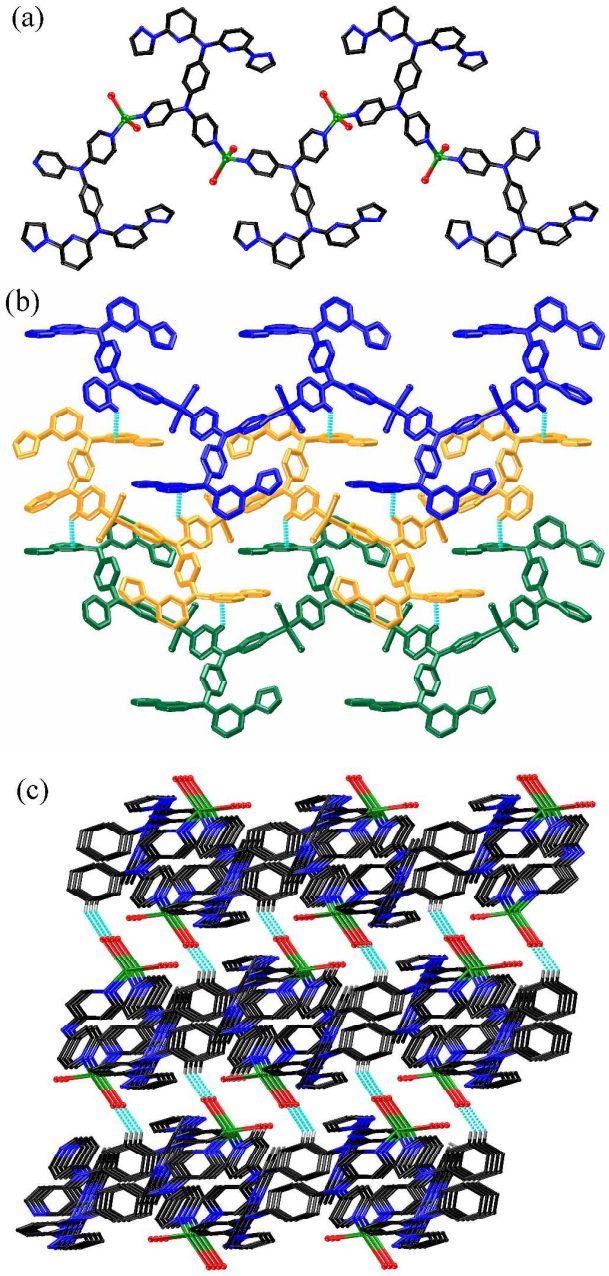

Fig 3. (a) 1D chain of complex **2**, (b) Two-dimensional network formed by interchain hydrogen bond interactions. (c) Three-dimensional supramolecular structure formed by hydrogen bond interactions.

2.436(5)~2.499(6) Å and the Cd-Cl bond length is 2.532(3) Å, which are comparable to those observed in similar complexes.[15]

In complexes **4** and **5**, L also adopts the "L" conformation and utilizes its pyridyl nitrogens of the 4,4'-dpa moieties to bridge Cd(II) atoms. Two head to head ligands link two Cd(II) atoms, affording a 20-membered metallomacrocycle, which are further linked to form a 1D double chain (Fig. 4a). And neighboring chains are further linked by intermolecular C–H···N hydrogen bonds between the pyrazolyl moieties. The C···N and H···N distances are 3.385(1) and 2.68 Å, respectively. The C–H···N angle is 134˚. Moreover, adjacent chains are almost perpendicular to each other. Finally, an undulated 2D layer is formed (Fig. 4b).

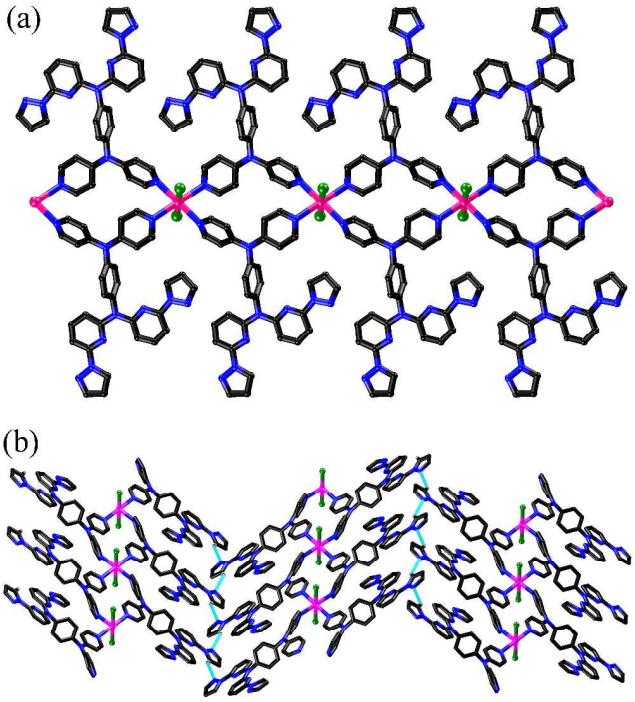

Fig 4. (a) 1D chain of complex **4**, (b) Two-dimensional network formed by linkage of interchain hydrogen bonds.

Crystal structure of $\{[CoL(SCN)](ClO_4)\}_n \cdot 1.5nDMF \cdot 0.5nH_2O$ (7). In complexes **1-6**, the L ligand adopts coordination modes of I or II (Scheme 4), with the bppa moieties left noncoordinated. In order to fully utilize the chelating units, we tried to use the paramagnetic Co(II) salts in place of the Zn(II) and Cd(II) salts to coordinate with L to afford complex **7**. Interestingly, the bppa units in complex **7** really chelate the Co(II) atoms, which is in sharp contrast to those observed in complexes **1**~**6**. Each Co(II) center adopts the six-coordinated octahedral geometry. The equatorial plane is composed of four nitrogen atoms from the chelating bppa units with the N-Co-N angles varying in the range of 79.37(15)~111.96(15)˚. The axial positions are occupied by one pyridyl nitrogen atom from an adjacent L ligand and one isothiocyanate nitrogen atom, with the N-Co-N angle of 177.72(15)˚, which indicates that Co locates in a slightly distorted octahedral coordination geometry. The Co–N bond lengths lie in the range of 2.085(4)~2.244(4) Å, which is consistent with the reported Co-N bond lengths of Co(II) complexes.[16]

In complex **7**, the bppa unit of L adopts the "U" conformation with two vertical branches chelating one Co(II) atom (Fig.5a). Meanwhile, one pyridyl nitrogen of the 4,4'-dpa unit bridges another Co(II) atom (mode III, Scheme 4), thus, affording a 1D chain structure (Fig.5a). Furthermore, the pyrazolyl C-H groups of the bppa units participate in weak C–H···S hydrogen bonds with the isothiocyanate sulfur atoms from the neighboring chain. The average C···S and H···S distances are 3.690(2) and 2.86 Å, respectively. The angle of C-H···S is 150˚. By linkage of the interchain H bonds, a 2D layer is formed (Fig. 5b).

Crystal structure of $\{[Cu_2L_2(N_3)]\cdot 3ClO_4\}_n$ (8)

Complex **8** was synthesized from the reaction of L and $Cu(ClO_4)_2 \cdot 6H_2O$ in the presence of NaN_3. As shown in Fig. 6a, each Cu(II) is six-coordinated with a slightly distorted octahedral geometry. Four nitrogen atoms from a bppa unit are coordinated

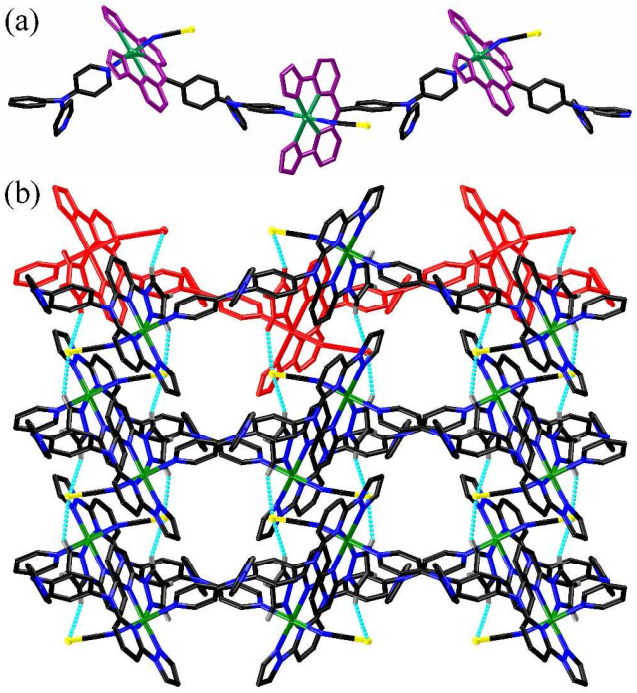

Fig 5. (a) 1D chain of complex **7**, (b) Two-dimensional network formed by interchain hydrogen bonds.

in the equatorial plane with the Cu-N bond lengths varying in the range of 1.971(3)~1.990(3) Å, and the axial positions are occupied by one $\mu_{1,3}$-azido group and one pyridyl nitrogen with the Cu-N bond lengths of 2.546(5) and 2.433(3) Å, respectively.

Similar to complex **7**, the bppa unit of ligand L in complex **8** also adopts the "U" conformation and chelates Cu(II) atoms. Thus, each L ligand links two Cu(II) ions and each Cu(II) ion links two L ligands, resulting in the formation of a 1D chain (Fig. 6b). Different from the terminally coordinated isothiocyanates in complex **7**, the $\mu_{1,3}$-azido moiety bridges two copper atoms from the adjacent chains, affording a 2D undulated layer (Fig. 6b). Topologically, each Cu atom can be considered as a three-connected node. Thus the 2D layer can be described as a uninodal 6^3-**hcb** net, which is interpenetrated by another such net, affording a 2-fold interpenetrated structure (Fig. 6c).

Coordination of ligand L and complex structural diversity

In the crystal structures of complexes **1-8**, the ligand L, combining the bridging 4,4'-dpa moiety and the chelating bppa moiety, adopts three different conformations (Scheme 4), affording a series of 1D and 2D coordination polymers, which indicates that L is an excellent ligand to assemble unique supramolecular structures.

Coordination polymers **1**–**6** were prepared by the coordination of ligand L with d^{10} metal ions Zn(II) and Cd(II). On the other hand, **7** and **8** were prepared in the presence of paramagnetic metal ions Co(II) and Cu(II). It is noteworthy that the bppa units of L effectively chelate the paramagnetic metal ions, in contrast, they are left noncoordinated in the d^{10} metal coordination polymers **1**-**6**. The results reveal that the bppa units can selectively chelate the paramagnetic Co(II) and Cu(II) metal ions, which may be rationalized by the cooperative effect of the radius and the coordination preferences of the metal ions. Zn^{2+} tends to form tetrahedral complexes.[17] Thus, it is rather unsuitable to chelate

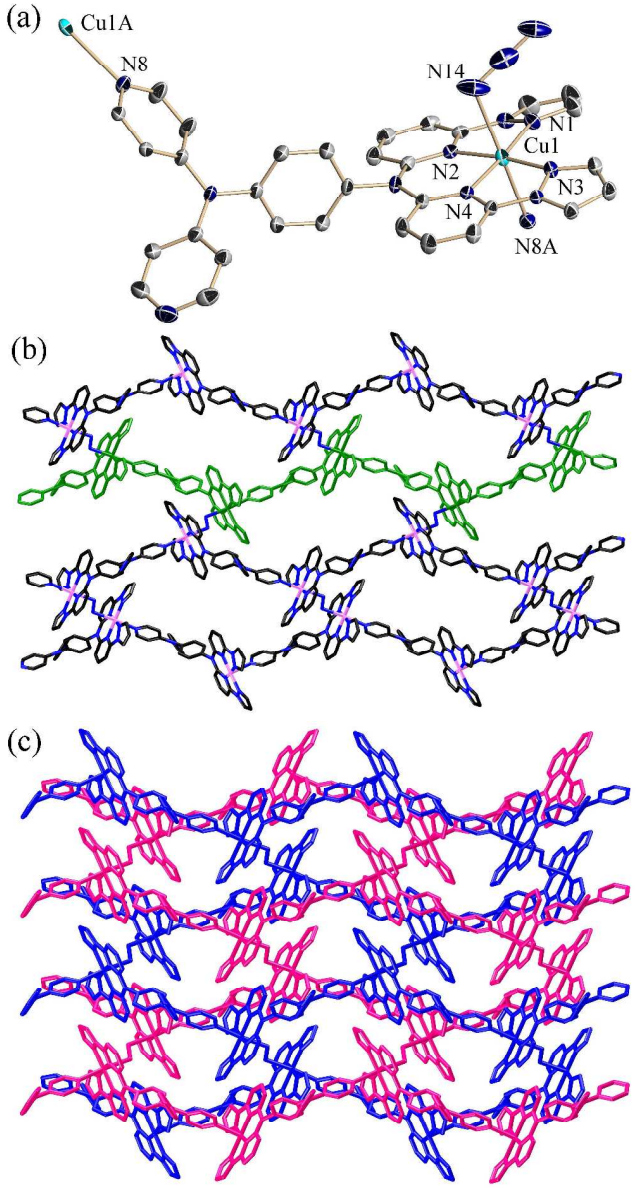

Fig 6 (a) View showing coordination environments of the Cu(II) centers in complex **8** with thermal ellipsoids shown at the 30% probability level. Perchlorates have been omitted for clarity. Symmetry operations, A: x, -y+1, z+1/2. (b) 2D network of complex **8**, (c) A 2-fold interpenetrated 2D structure.

the bppa moiety. Accordingly, noncoordinated bppa moieties were observed in complexes **1**~**3**. On the other hand, Co(II) and Cu(II) metal ions tend to form octahedral complexes,[18] and thus the bppa moieties are observed to chelate in the equatorial planes of the octahedral Co(II) and Cu(II) centers in complexes **7** and **8**, respectively. Similar to Co(II) and Cu(II), Cd^{2+} also tends to form octahedral complexes,[19] which can be observed from the crystal structures of **4** and **5**. In spite of this, the radius of Cd(II) is significantly larger than those of Co(II) and Cu(II). And thus, the Cd(II) center cannot be chelated within the bppa moiety. Hence, the N atoms from the 4,4′-dpa moieties were observed to bridge the Cd(II) centers in the equatorial plane.

It is noteworthy that three different conformations are observed for the bppa moieties. In complexes **7** and **8**, the chelating bppa moieties adopt the "U"-shape conformation. In complexes **1**~**6**, the noncoordinated bppa units adopt either the "L" or the "M" conformation, and the difference may be related to weak intermolecular interactions. Thus, the structural diversity of the complexes may be partly ascribed to the conformational flexibility of the bppa unit.

For cadmium complexes **4**-**6**, the changes of the anions cause the structural diversity. In complexes **4** and **5**, the ligands are linked by Cd(II) atoms in the "head to head" mode, affording a 1D chain structure. When the iodine anion is used to replace the chlorine and bromine anions, the cadmium atom adopts the tetrahedral coordination geometry, affording a 1D zigzag chain structure. Apparently, the anions have been observed to remarkably influence the structures of the coordination polymers. Besides, in the syntheses of coordination polymers **7** and **8**, SCN^- and N_3^- groups are used as the ancillary ligands. As described above, both **7** and **8** have similar chain structures formed by the bridging and chelating of L. In complex **7**, the ancillary SCN^- coordinates only as a terminal ligand. In contrast to this observation, the N_3^- group in complex **8** bridges the copper atoms from two neighboring chains, thus affording a 2D net. These results indicate that the bridging ancillary ligands may provide opportunities for the building of higher-dimensional structures.

In summary, the diverse complex structures were obtained thanks to the coordination and conformational flexibility of the L ligand, in combination with several other important factors, such as the metal atoms, the anions, and the ancillary ligands.

Photoluminescence

Coordination polymers with d^{10} metal centers have been reported to exhibit solid state emissions with easily modulated intensities and wavelengths.[20-21] Hence, the photoluminescent properties of the ligand L and complexes **1**~**6** were investigated in the solid state at room temperature (Fig. 7). The free ligand L exhibits an intense emission band centered at 387 nm upon excitation at 320 nm, which may be attributed to the $\pi^* \rightarrow \pi$ transition.[22]

As mentioned above, the structures of complexes **1**-**6** can be divided into following two categories: (I) 1D zigzag-like chains for complexes **1**-**3** and **6**; and (II) 1D double chains for complexes **4** and **5**. For the first type of complexes **1**-**3** and **6**, the emission bands are observed at 453, 486, 406 and 407 nm, respectively. These bands are red-shifted, as compared with that of 387 nm for the ligand. For the second type, complexes **4** and **5** have broad emission bands centered at 386 and 372 nm, respectively. These bands are blue-shifted as compared to that of L. Due to the similarity of the emission bands with that of L, the emissions of complexes **1**-**6** may be attributed to the intraligand transitions.[23] Furthermore, it may be concluded that the zigzag chain mode can decrease the HOMO−LUMO energy gap of the ligand L with the red-shifted emission wavelength. In contrast, the double chain mode can induce slight increase of the HOMO−LUMO energy gap. It is obvious that the changes in the coordination modes can greatly influence the emission wavelengths.[24]

Although complexes **1**-**3** have the same metal ions and similar crystal structures, their emission wavelengths vary in the range of 406~486 nm, which may be ascribed to the difference in the coordinated anions, because photoluminescent behavior is closely

related to the local environments around the metal ions.[25] It is also noteworthy that the fluorescence intensities for **2** and **3** are weaker than that of **1**, which may be related to the heavy atom effect.[26] In summary, the emission behavior can be well tuned, with the emission maxima varying in the range of 372 ~ 486 nm.

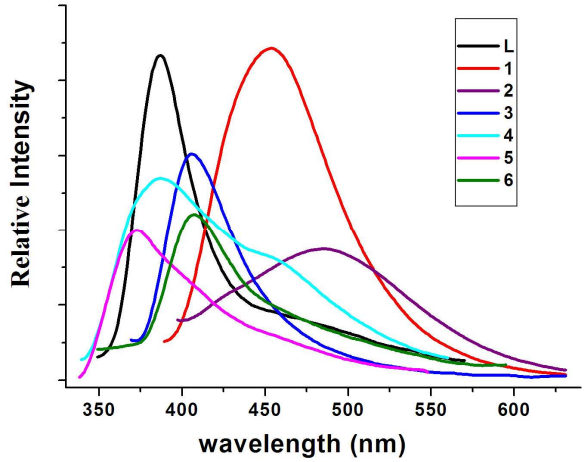

Fig. 7. Emission spectra of L and complexes **1**−**6** in the solid state at room temperature.

Conclusions

A novel ligand L containing the bridging 4,4'-dpa unit and the chelating bppa unit was synthesized and used to coordinate with d^{10} metals, including Zn(II), Cd(II) to affording coordination polymers **1**~**6**. Complexes **1**-**3** and **6** demonstrate isostructural 1D zigzag chain structures, and complexes **4** and **5** have 1D double chain structures. In these six complexes, the chelating bppa units are left non-coordinated in the "L" or "M" conformation. However, when Co(II) and Cu(II) salts were used to coordinate with L, these metal ions were successfully chelated by the bppa units to afford coordination polymers **7** and **8**, with the bppa unit coordinated in the "U" conformation. These results indicate that the ligand L can selectively chelate paramagnetic metal ions. Furthermore, the solid state photoluminescence of L and complexes **1**-**6** was measured. and discussed based on the structural results. The emission maxima wavelengths can be tuned in a large range of 372−486 nm.

Acknowledgements

This work was financially supported by NSFC (21072060, 91227201), the Program for Professor of Special Appointment (Eastern Scholar) at Shanghai Institutions of Higher Learning, Program for New Century Excellent Talents in University (NCET-11-0638), the Fundamental Research Funds for the Central Universities (WK1013002), and SRFDP (20100074110015).

References

1 (a) Q. Li, W. Zhang, O. Š. Miljanić, C. H. Sue, Y. L. Zhao, L. Liu, C. B. Knobler, J. F. Stoddart, O. M. Yaghi, *Science,* 2009, **325**, 855. (b) D. Han, F. L. Jiang, M. Y. Wu, L. Chen, Q. H. Chen, M. C. Hong, *Chem. Commun.* 2011, **47**, 9861.(c) W. Xuan, M. Zhang, Y. Liu, Z. Chen, Y. Cui, *J. Am. Chem. Soc.,* 2012, **134**, 6904.(d) H. B. Xu, B. W. Wang, F. Pan, Z. M. Wang, S. Gao, *Angew. Chem., Int. Ed.* 2007, **46**, 7388.

2 (a) Z. Zhang, L. Zhang, L. Wojtas, P. Nugent, M. Eddaoudi, M. J. Zaworotko, *J. Am. Chem. Soc.,* 2012, **134**, 924. (b) J. F. Guo, X. T. Wang, B. W. Wang, G. C. Xu, S. Gao, L. Szeto, W. T. Wong, W. Y. Wong, T. C. Lau, *Chem.-Eur. J.* 2010, **16**, 3524. (c) M. X. Li, Z. X. Miao, M. Shao, S. W. Liang, S. R. Zhu, *Inorg. Chem.,* 2008, **47**, 4481.(d) G. Li, W. B. Yu, Y. Cui, *J. Am. Chem. Soc.,* 2008, **130**, 4582. (e) Y. B. Zhang, W. X. Zhang, F. Y. Feng, J. P. Zhang, X. M. Chen, *Angew. Chem., Int. Ed.* 2009, **48**, 5287.

3 (a) J. P. Hill, N. K. Subbaiyan, F. D'Souza, Y. S. Xie, S. Sahu, S N. M. anchez-Ballester, G. J. Richards, T. Mori, K. Ariga, *Chem. Commun.,* 2012, **48**, 3951.(b) X. Xi, T. Dong, G. Li, Y. Cui, *Chem. Commun.,* 2011, **47**, 3831. (c) G. Novitchi, G. Pilet, L. Ungur, V. V. Moshchalkov, W. Wernsdorfer, L. F. Chibotaru, D. Luneau, A. K. P owell, *Chem. Sci.,* 2012, **3**, 1169. (d) J. P. Hill, H. Palza, S. Alam, K. Ariga, A. L. Schumacher, F. D'Souza, C. E. Anson, A. K. Powell, *Inorg. Chem*. 2008, **47**, 8306..

4 (a) J. An, C. M. Shade, D. A. Chengelis-Czegan, S. p. Petoud, N. L. Rosi, *J. Am. Chem. Soc.,* 2011, **133**, 1220. (b) K. H. He, W. C. Song, Y. W. Li, Y. Q. Chen, X. H. Bu, *Cryst.Growth & Des.* 2012, **12**, 1064. (c) S. Q. Bai, C. J. Fang, Z. He, E. Q. Gao, C. H. Yan, T. S. A. Hor, *CrystEngComm* 2013, **15**, 650.

5 (a) Y. P. He, Y. X. Tan, F. Wang, J. Zhang, *Inorg. Chem.* 2012, **51**, 1995. (b) Q. Hua, Y. Zhao, G. C. Xu, M. S. Chen, Z. Su, K. Cai, W. Y. Sun, *Cryst.Growth Des.* 2010, **10**, 2553. (c) P. Lama, P. K. Bharadwaj, *Cryst.Growth Des.* 2011, **11**, 5434.

6 (a) S.M. Li, X. J. Zheng, D. Q. Yuan, A. Ablet, L. P. Jin, *Inorg. Chem.* 2012, **51**, 1201. (b) K. K. Tanabe, C. A. Allen, S. M. Cohen, *Angew. Chem., Int. Ed.* 2010, **49**, 9730. (c) R. Feng, F. L. Jiang, L. Chen, C. F. Yan, M. Y. Wu, M. C. Hong, *Chem. Commun.* 2009, 5296. (d) H. Wang, D. Qi, Z. Xie, W. Cao, K. Wang, H. Shang, J. Jiang, *Chem. Commun.* 2013, **49**, 889.

7 (a) C. J. Sumby, *Coord. Chem. Rev.* 2011, **255**, 1937. (b) J. H. Kuo, T. B. Tsao, G. H. Lee, H. W. Lee, C. Y. Yeh, S. M. Peng. *Eur. J. Inorg. Chem.* 2011, 2025. (c) X. T. Wang, X. H. Wang, Z. M. Wang, S. Gao, *Inorg. Chem.* 2009, **48**, 1301. (d) G. A. Farnum, J. H. Nettleman, R. L. LaDuca, *CrystEngComm* 2010, **12**, 888. (e) L. K. Sposato, J. H. Nettleman, M. A. Braverman, R. M. Supkowski, R. L. LaDuca, *Cryst. Growth Des.* 2010, **10**, 335.

8 (a) R. L. LaDuca, *Coord. Chem. Rev.* 2009, **253**, 1759. (b) Z. M. Hao, X. M. Zhang, *Cryst. Growth Des.*, 2007, **7**, 64. (c) K. J. Wei, Y. S. Xie, J. Ni, M. Zhang, Q. L. Liu, *Cryst. Growth Des.*, 2006, **6**, 1341. (d) Q. G. Wang, Y. S. Xie, F. H. Zeng, S. W. Ng, W. H. Zhu, *Inorg. Chem. Commun.* 2010, **13**, 929.

9 (a) F. H. Zeng, J. Ni, Q. G. Wang, Y. B. Ding, S. W. Ng, W. H. Zhu, Y. S. Xie, *Cryst. Growth Des.*, 2010, **10**, 1611. (b) C. Ding, X. Li, Y. Ding, X. Li, S. W. Ng, Y. Xie, *Cryst. Growth Des.*, 2012, **12**, 3465. (c) Q. Z. Zha, C. X. Ding, X. Rui, Y. S. Xie, *Cryst. Growth Des.* 2013, **13**, 4583.

10 Y. S. Xie, Y. B. Ding, X. Li, C. Wang, J. P. Hill, K. Ariga, W. B. Zhang, W. H. Zhu, *Chem. Commun.* 2012, **48**, 11513.

11 (a) G. M. Sheldrick, SHELXS97 and SHELXL97 Programs for Crystal Structure Solution and Refinement, University of Göttigen, Germany, 1997. (b) G.M. Sheldrick, *Acta Cryst.,* 2008, **A64**, 112.

12 (a) K. Nakamoto, in *Infrared and Raman Spectra of Inorganic and Coordination Compounds*; John Wiley & Sons, Inc.: Hoboken, NJ, 2008, Chapter 1, pp 121-126. (b) M. X. Li, H. Wang, S. W. Liang, M. Shao, X. He, Z. X. Wang, S. R. Zhu, *Cryst. Growth Des.,* 2009, **9**, 4626. (c) J. C. Jiang, Z. L. Chu, W. Huang, G. Wang, X. Z. You, *Inorg. Chem.,* 2010, **49**, 5897;

13 A. Bondi, *J. Phys. Chem.* 1964, **68**, 441.

14 (a) Z. W. Yang, X. J. Huang, Q. L. Zhao, S. G. Li, B. A. Wu, *CrystEngComm* 2012, **14**, 5446. (b) N. N. Adarsh, P. Dastidar, *Cryst.Growth Des.* 2011, **11**, 328.

15 (a) P. Cui, Z. Chen, D. Gao, B. Zhao, W. Shi, P. Cheng, *Cryst.Growth Des.* 2010, **10**, 4370. (b) Y. L. Jiang, Y. L. Wang, J. X. Lin, Q. Y. Liu, Z. H. Lu, N. Zhang, W. Jia Jia, L. Q. Li, *CrystEngComm* 2011, **13**, 1697. (c) G. Q. Kong, C. D. Wu, *CrystEngComm* 2012, **14**, 847.

16 (a) Y. Q. Tian, C. X. Cai, X. M. Ren, C. Y. Duan, Y. Xu, S. Gao, X. Z. You, *Chem.- Eur. J.* 2003, **9**, 5673. (b) J. Olguín, M. Kalisz, R. Clérac,

S. Brooker, *Inorg. Chem.* 2012, **51**, 5058.

17 (a) L. Luo, K. Chen, Q. Liu, Y. Lu, T. A. Okamura, G. C. Lv, Y. Zhao, W. Y. Sun, *Cryst. Growth Des.* 2013, **13**, 2312. (b) A. Schaate, S. Klingelhöfer, P. Behrens, M. Wiebcke, *Cryst. Growth Des.* 2008, **8**, 3200. (c) J. Gao, N. Wang, X. Xiong, C. Chen, W. Xie, X. Ran, Y. Long, S. Yue, Y. Liu, *CrystEngComm* 2013, **15**, 3261.

18 (a) C. X. Ding, J. Ni, Y. H. Yang, S. W. Ng, B. W. Wang, Y. S. Xie, *CrystEngComm* 2012, **14**, 7312. (b) Y. S. Xie, J. Ni, F. K. Zheng, Y. Cui, Q. G. Wang, S. W. Ng, W. Zhu, *Cryst. Growth Des.* 2009, **9**, 118. (c) Y. Y. Tang, C. X. Ding, S. W. Ng, Y. S. Xie, *RSC Adv.* 2013, **3**, 18134.

19 (a) J. W. Shin, J. M. Bae, C. Kim, K. S. Min, *Inorg. Chem.* 2013, **52**, 2265. (b) X. Li, X. Guo, X. Weng, S. Lin, *CrystEngComm* 2012. **14**, 1412. (c) Z. Su, K. Cai, J. Fan, S. S. Chen, M. S. Chen, W. Y. Sun, *CrystEngComm* 2010, **12**, 100.

20 (a) L. Bergmann, J. Friedrichs, M. Mydlak, T. Baumann, M. Nieger, S. Brase, *Chem. Commun.* 2013, **49**, 6501. (b) Y. Gong, P. G. Jiang, J. Li, T. Wu, J. H. Lin, *Cryst.Growth Des.* 2013, **13**, 1059. (c) D. M. Zink, M. Bächle, T. Baumann, M. Nieger, M. Kühn, C. Wang, W. Klopper, U. Monkowius, T. Hofbeck, H. Yersin, S. Bräse, *Inorg. Chem.* 2013, **52**, 2292.

21 (a) L. Croitor, E. B. Coropceanu, A. V. Siminel, V. C. Kravtsov, M. S. Fonari, *Cryst.Growth Des.* 2011, **11**, 3536. (b) J. Cui, Q. Yang, Y. Li, Z. Guo, H. Zheng, *Cryst. Growth Des.* 2013. **13**, 1694. (c) M. Maiti, D. Sadhukhan, S. Thakurta, S. Roy, G. Pilet, R. J. Butcher, A. Nonat, L. J. Charbonniere, S. Mitra, *Inorg. Chem.* 2012, **51**, 12176.

22 (a) X. Shi, G. S. Zhu, Q. R. Fang, G. Wu, G. Tian, R.W. Wang, D. L. Zhang, M. Xue, S. L. Qiu, *Eur. J. Inorg. Chem.* 2004, 185. (b) G. Tian, G. S. Zhu, Q. R. Fang, X. D. Guo, M. Xue, J. Y. Sun, S. L. Qiu, *J. Mol. Struct*. 2006, **787**, 45.

23 (a) L. J. Chen, X. He, C. K. Xia, Q. Z. Zhang, J. T. Chen, W. B. Yang, C. Z. Lu, *Cryst. Growth Des.* 2006, **6**, 2076. (b) C. Xu, Q. Guo, X. Wang, H. Hou, Y. Fan, *Cryst. Growth Des.* 2011, **11**, 1869. (c) B. X. Dong, Q. Xu, *Cryst. Growth Des*. 2009, **9**, 2776.

24 (a) N. Kundu, S. M. Abtab, S. Kundu, A. Endo, S. J. Teat, M. Chaudhury, *Inorg. Chem.* 2012, **51**, 2652. (b) J. W. Shin, J. M. Bae, C. Kim, K. S. Min, *Inorg. Chem.* 2013, **52**, 2265.(c) G. C. Xu, L. Zhang, Y.-H. Zhang, J. X. Guo, M. Q. Shi, D. Z. Jia, *CrystEngComm* 2013, **15**, 2873.

25 (a) Z. Y. Fu, X. T. Wu, J. C. Dai, S. M. Hu, W. X. Du, H. H. Zhang, R. Q. Sun, Eur. J. *Inorg. Chem*. 2002, 2730. (b) L. L. Wen, D. B. Dang, C. Y. Duan, Y. Z. Li, Z. F. Tian, Q. J. Meng, *Inorg. Chem.* 2005, **44**, 7161. (c) Y. N. Zhang, P. Liu, Y. Y. Wang, L. Y. Wu, L. Y. Pang, Q. Z. Shi, *Cryst. Growth Des*. 2011, **11**, 1531.

26 (a) R. S. Drago, Physical Methods in Chemistry; Saunders: Philadelphia, 1977; Chapter 5. (b) F. Masetti, U. Mazzucato, G. J. Galiazzo, *Lumin.* 1971, **4**, 8. (c) T. C. Warner, W. Hawkins, J. Facci, R. Torrisi, T. Trembath, *J. Phys. Chem*. 1978, **82**, 298. (d) M. C. Aragoni, M. Arca, F. Demartin, F. A. Devillanova, F. Isaia, A. Garau, V. Lippolis, F. Jalali, U. Papke, M. Shamsipur, L. Tei, A. Yari, G. Verani, *Inorg. Chem.* 2002, **41**, 6623. (e) C. Seward, J. Chan, D. Song, S. N. Wang, *Inorg. Chem*. 2003, **42**, 1112.

For Table of Contents Entry Use Only

Coordination Polymers of a Multipyridyl and Pyrazolyl Ligand with Conformational Flexibility: Syntheses, Structures and Luminescence

Caixia Ding, Xing Rui, Cheng Wang and Yongshu Xie

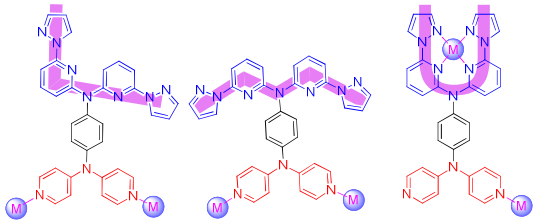

Eight novel coordination polymers were obtained by the coordination of a multipyridyl and pyrazolyl ligand, which shows rich conformational changes.